Smart Structures and Systems, Vol. 7, No. 5 (2011) 349-363
DOI: http://dx.doi.org/10.12989/sss.2011.7.5.349

Monitoring a steel building using GPS sensors

Fabio Casciati* and Clemente Fuggini

Department of Structural Mechanics, University of Pavia, via Ferrata 1, 27100, Pavia, Italy

(Received December 8, 2009, Accepted January 13, 2011)

Abstract. To assess the performance of a structure requires the measurement of global and relative displacements at critical points across the structure. They should be obtained in real time and in all weather condition. A Global Navigation Satellite System (GNSS) could satisfy the last two requirements. The American Global Position System (GPS) provides long term acquisitions with sampling rates sufficient to track the displacement of long period structures. The accuracy is of the order of sub-centimetres. The steel building which hosts the authors' laboratory is the reference case-study within this paper. First a comparison of data collected by GPS sensor units with data recorded by tri-axial accelerometers is carried out when dynamic vibrations are induced in the structure by movements of the internal bridge-crane. The elaborations from the GPS position readings are then compared with the results obtained by a Finite Element (FE) numerical simulation. The purposes are: i) to realize a refinement of the structural parameters which characterize the building and ii) to outline a suitable way for processing GPS data toward structural monitoring.

Keywords: global positioning systems; sensors; structural dynamics; structural identification; vibration.

1 Introduction

Within any Structural Health Monitoring (SHM) scheme in civil and infrastructure engineering, accuracy, durability and availability are basic requirements to satisfy in view of feasible and reliable long-term applications (Sumitro and Wang 2005).

Structural monitoring requires the collection of absolute and relative displacements at critical points across the structural systems. Indeed, the relative displacements are the key to assess drift and stress conditions in a structure, toward the evaluation of a suitable index of its health condition. The availability of real-time data is then a need in view of producing alert messages and modifying the maintenance activities. The availability of the monitoring system under negative atmospheric conditions or large temperature variations is also a basic requirement.

In the last few years Global Navigation Satellites Systems (GNSS) have been proved useful for monitoring applications in structural engineering. They guarantee operability in all weather conditions, offer continuous long term acquisitions and provide absolute and relative displacements directly. Among the satellite positioning systems (American, Russian and the future European), the American Global Positioning System (GPS) can be regarded as an alternative to common accelerometers in different types of monitoring applications.

GPS sensors have been experimentally tested to measure the dynamic response of long-period

*Corresponding Author, Professor, E-mail: fabio@dipmec.unipv.it

structures (Celebi 2006, Nickitopoulou *et al*. 2006, Kijewsji *et al.* 2006, Li *et al.* 2006, Psimoulis *et al.* 2008); to monitor the wind-induced deformation of tall flexible buildings (Kijewsji-Correa and Kareem 2003, Campbell *et al.* 2006, Seco *et al.* 2007, Hristopulos *et al.* 2007); to asses the vibrations of suspension and cable-stayed bridges (Xu *et al.* 2002, Lekidis *et al.* 2005, Meng *et al.* 2007), the displacements of high chimneys (Breuer *et al.* 2002, Cazzaniga and Pinto 2006) and large dams (Barnes *et al.* 2006). Many applications were developed by installing GPS receivers at key locations of the structure to capture their static and dynamic displacements in real time and in all weather conditions (Tamura *et al.* 2002). In other cases, GPS units were incorporated in the monitoring of a major suspension bridge (Wong 2004), or of tall structures (Psimoulis and Stiros 2008, Ni *et al*. 2009).

The accuracy of such an approach to measure tri-dimensional displacements is deeply discussed in the literature (see (Celebi 2000, Nickitopoulou *et al.* 2006, Kijewsji-Correa *et al.* 2006, Psimoulis *et al*. 2008, Tamura *et al.* 2002, Psimoulis and Stiros 2008, Ni *et al*. 2009), among others).

Recently the authors have been investigating the effectiveness of a full-scale GPS monitoring. Different aspects were considered:

1) the reliability of the GPS in collecting static and dynamic 3D movements of monitored points for real time measurements was assessed (Casciati and Fuggini 2009)
2) the uncertainty of the measurements (due to sensors placement, structural identification and diagnostic processes) was quantified (Casciati and Fuggini 2009)
3) a comparison of GPS data with those recorded by tri-axial accelerometers was carried out under dynamic vibrations (Casciati and Fuggini 2009).

The feasibility of a structural monitoring scheme adopting a GPS network still claims for full scale implementations. The steel building which hosts the authors' laboratory was chosen as a potential case study. Man-made (i.e., produced by movements of the internal bridge crane) dynamic actions are considered. First a comparison of the GPS records with those collected by tri-axial accelerometers is conducted. A numerical simulation using a finite element (FE) model of the building is then developed and the elaborations from the GPS position readings are compared with the simulation results. The main purpose of this task is to refine the parameters of the structural model of the building.

2. GPS network architecture

The system architecture is made of an outdoor part, consisting of antennas (of height 6.2 cm, diameter 17.0 cm of and mass 0.4 Kg), and an indoor part assembling the receivers and a computer running a Leica software product. The devices installed are (Leica 2005):

- One dual frequency high precision Leica GMX902 GPS receiver, working as reference , with a maximum sampling rate of 20 Hz;
- Two dual frequency high precision Leica GMX1200 GPS receivers, working as rovers, with a maximum sampling rate of 20 Hz;
- Three dual frequency Leica AX1202 antennas, recording signal with a sampling rate up to 20Hz.

It is worth noting that the sampling rate of 20Hz is not the result of a choice by the authors. It is simply the upper limit offered by the commercial units the market offers.

The GPS signals are recorded by the Leica GPS Spider software that furnishes information on the satellites configuration and allows corrections of data for a real time positioning. The recorded displacement signals are then analyzed using a system identification toolbox (Matlab 2004).

The moving antenna and the fixed antenna are linked to their receivers by wire connections, and other wires connect the receivers to a computer for the acquisition of the GPS signals. Dual frequency L1/L2 GPS receivers are used to guarantee the maximum achievable accuracy. The rovers and the reference receivers communicate each to the other to allow the correction of position errors, according to the *Differential Global Positioning System (DGPS)* scheme (Dana 1997).

Preliminary static and dynamic calibration tests were carried out and their results were presented elsewhere (Casciati and Fuggini 2009, Casciati *et al.* 2007, Fuggini 2010). The static tests allow to quantify the background noise in the GPS configuration, and to investigate the influence of the signal Geometric Dilution of Precision (GDOP). It is mainly due to a deviation from the idealized geometric distribution of the satellites and can be modelled by a geometric factor which describes the effect of the actual geometric satellites distribution on the accuracy of the target position. The static tests provide answers to two main questions: a) repeatability of long-period oscillations in both the longitudinal and transversal directions for two consecutive satellite configurations; b) evaluation of the highest possible resolution when adopting dual frequency GPS receivers.

The dynamic tests have been designed to quantify the range of frequencies and amplitudes that can be successfully tracked by GPS sensors in Civil Engineering applications.

This preliminary phase was also useful to collect any possible information in view of assessing the achievable accuracy of the GPS units for long-term precise monitoring applications. Furthermore, it provided information on how the GPS data have to be processed in view of their use within an identification scheme.

3. The experimental mock-up

Three GPS antennas have been placed on the roof of the industrial steel building (Fig. 1) in Pavia, at the height of about 11 m (i.e., on the top of the lower roof in Fig. 1), in an open field location free from sources of multi-paths errors and from buildings that may obstruct the view of the low elevation satellites (Casciati *et al.* 2007, Casciati and Fuggini 2008).

The building is a steel structure made of three blocks: it is 81 m long in the longitudinal direction (Y) and 64.5 m in the transversal one (X). The weight-bearing element is a 2D Pratt truss, which connects, the columns along the longitudinal direction. Transversal links along the transversal direction are repeated every 5.4 m. Perimeter wind-braces are also mounted (Fig. 2).

In each sensor placement, one antenna is fixed, and the others are movable. The fixed unit, (at the height of 13 m) marked in the following as "*a*", makes simultaneously the position correction for

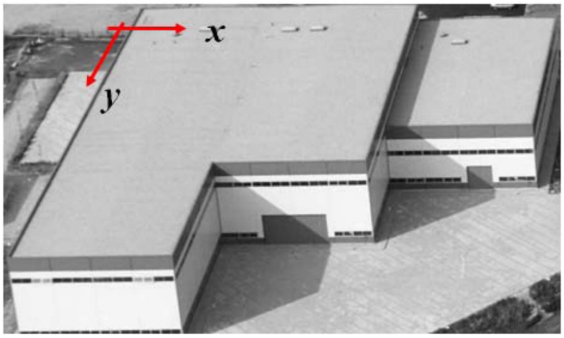

Fig. 1 Bird flight view of the industrial building in Pavia

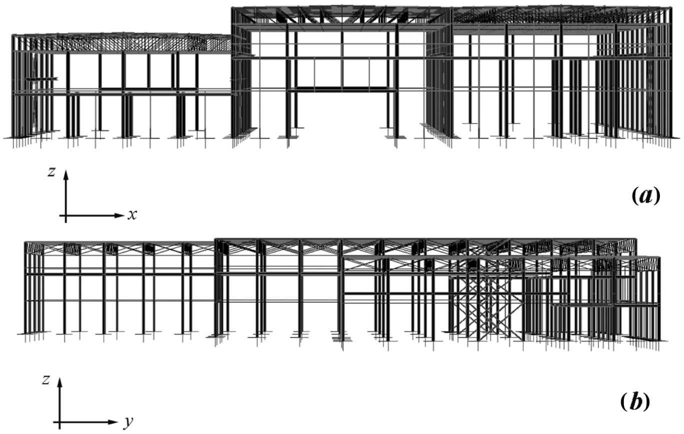

Fig. 2 Internal view of the building: front side (a) and lateral side (b)

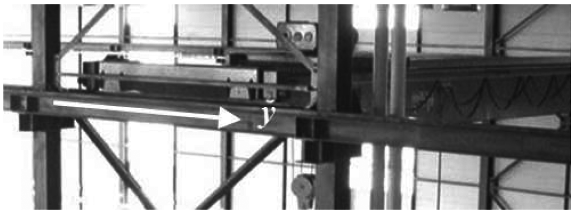

Fig. 3 The bridge-crane inside the building

both the movable receivers "*b*" and "*c*" (at the height of 11 m). This is achieved by sending them a new position, purified by the errors (i.e., atmospheric effects) (Kaplan and Hegarty 2006).

The estimation of GPS precision is discussed for oscillations generated by movements of the internal bridge-crane (Fig. 3). The duration of the recorded time histories is of a few seconds.

The critical point is to verify if GPS can detect sudden structural displacements due to reaction forces from bridge-crane movements. Elaborations from the GPS records are first compared with the signals obtained by standard tri-axial accelerometers. The same elaborations from the GPS position readings are then compared with the results obtained from a finite-element numerical simulation.

4. Tests and collected records

4.1 GPS unit placement

The GPS sensors' locations on the roof of the industrial steel building are shown in Fig. 4.

The sensors placement is chosen such as the baseline connecting the rover "*c*" (movable) with the reference "*a*" (fixed) is mainly oriented along the East direction, while the baseline connecting the two movable rovers "*b*" and "*c*" is mainly oriented along the North.

The East-North GPS reference system does not coincide with the *X* and *Y* axis of the Cartesian System chosen consistent with the direction of the bridge-crane movements along its rails (Fig. 4). A coordinate system transformation is introduced to calculate, from the East and North GPS recorded data, the displacement components along the *X* and *Y* axes, which denote the transversal

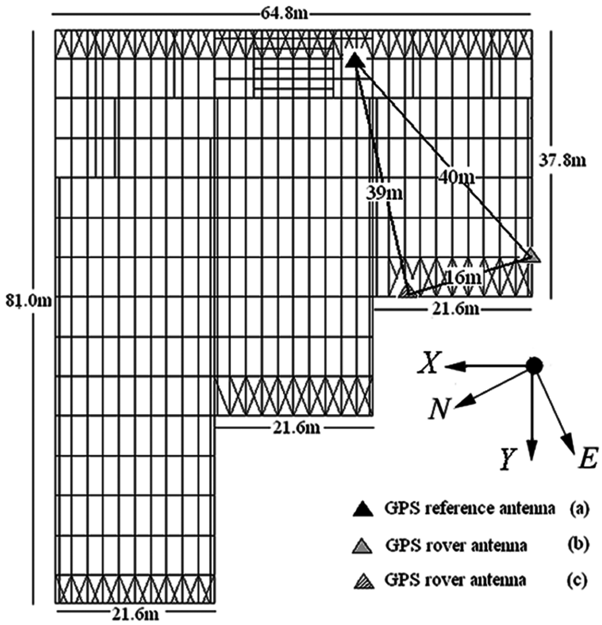

Fig. 4 GPS configuration in the *N-E* and *X-Y* plane. α is the angle between axes *X* and *N*

and the longitudinal direction of the building, respectively.

The coordinates transformation from the *N-E* Cartesian System to the *X-Y* one is made by adopting a suitable rotational matrix Γ such as presented in Eq. (1)

$$\begin{pmatrix} n \\ e \end{pmatrix} = \Gamma \begin{pmatrix} x \\ y \end{pmatrix} = \begin{bmatrix} \cos\alpha & \sin\alpha \\ -\sin\alpha & \cos\alpha \end{bmatrix} \begin{pmatrix} x \\ y \end{pmatrix} \tag{1}$$

which can be inverted to obtain the *x* and *y* coordinates

$$\begin{pmatrix} x \\ y \end{pmatrix} = \Gamma^{-1} \begin{pmatrix} n \\ e \end{pmatrix} = \begin{bmatrix} \cos\alpha & -\sin\alpha \\ \sin\alpha & \cos\alpha \end{bmatrix} \begin{pmatrix} n \\ e \end{pmatrix} \tag{2}$$

where α (=18,9°) represents the angle of rotation from the *X-Y* to the *N-E* Cartesian Systems.

The bridge-crane is mounted on rails running inside the steel building at the height of 8 m and covering a span of around 20 m. It allows three types of movements (Fig. 5):

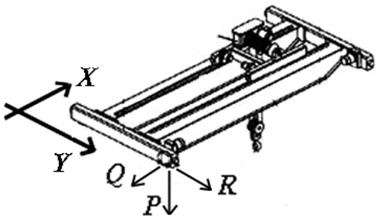

Fig. 5 Bridge-crane reaction forces in the *X-Y* plane

(i) vertical movements of the load, inducing a vertical reaction *P*
(ii) longitudinal horizontal movements (i.e., along its way beam), inducing a longitudinal reaction *R*
(iii) transversal displacements for horizontal movements of the load, inducing a transversal reaction *Q*.

Longitudinal backward and forward bridge-crane movements induce significant vibrations on the steel structure. The bridge-crane can be moved at the speed of 0.7 m/s. While the bridge-crane moves along the longitudinal direction (*Y*), the GPS devices placed on the roof record the frame oscillations. When the bridge-crane stops, at the end of its ride, a peak force (opposite to the reaction *R*) of 10.93 KN is generated, as from the producer's specification.

The obtained short duration records were processed focusing on two different objectives:

a) a comparison of the GPS displacements with those obtained by integrating the accelerations recorded by tri-axial accelerometers placed nearby the GPS antennas

b) the refinement of the parameters of the numerical model of the industrial building. For this purpose a FE model of the structure is realized, while the actual man-made actions (i.e., those resulting from the bridge-crane movements) are simulated.

The first aspect was already discussed in references (Casciati and Fuggini 2009). In that follows of this section, a new set of tests is reported, for the new GPS locations on the roof of the building (see Fig. 4). The second aspect is approached in Section 5.

4.2 Short duration records data processing

Two tri-axial Kinemetrics Episensor accelerometers were placed nearby each of the two GPS moving antennas (Fig. 6), where a single couple of sensors is shown, i.e., the cylindrical Episensor and the GPS antenna.

The accelerometers record, at a sampling rate of 100Hz, the accelerations in the *X* and *Y* directions when the bridge-crane is moving along its rails inside the building. The along *X* signal corresponds to the calculated GPS *X* component, while the along *Y* accelerometers record corresponds to the calculated GPS *Y* component. The accelerometer close to the GPS "*b*" is mentioned in the following as Acc. "*b*", while the accelerometer close to the GPS "*c*" is referred as Acc. "*c*".

For the purpose of a direct comparison, a double integration procedure is applied to the acceleration data measured by the accelerometers (and re-sampled at 10 Hz), in order to convert them into displacements and to compare the result with the displacements directly measured by the GPS sensors. Both signals are processed by a band-pass filter between 0.01 and 5 Hz. For the GPS,

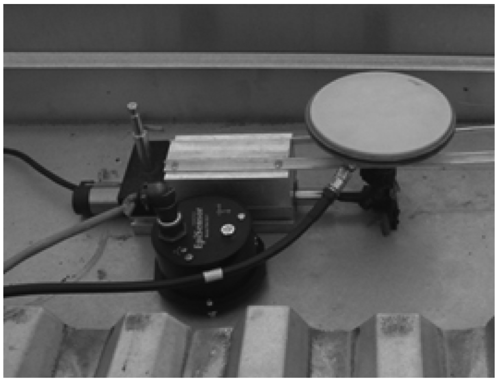

Fig. 6 View of the experimental setup

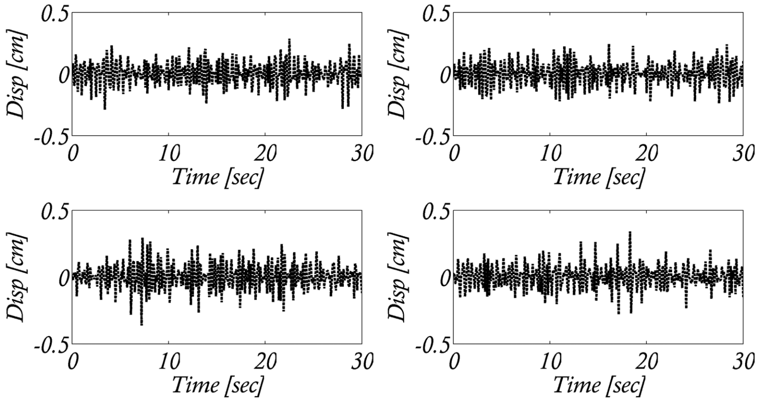

Fig. 7 GPS recorded displacements time histories along the X (left side plots) and Y axes (right side plots). Top: GPS "*c*" displacements. Bottom: GPS "*b*" displacements

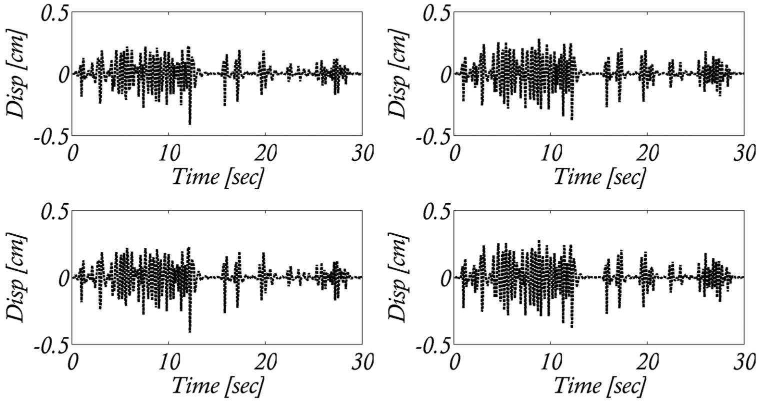

Fig. 8 Accelerometers calculated displacements time histories along the X (left side plots) and Y axes (right side plots). Top: Acc. "*c*" displacements. Bottom: Acc. "*b*" displacements

filtering very low frequencies is needed, as they are often associated to multi-path effects (Kijewsji-Correa *et al.* 2006).

Figs. 7 and 8 show the results for both the components X and Y. In Fig. 7, the top plot depicts the GPS displacement record for sensor "*c*", while the bottom plot provides the GPS displacement record for sensor "*b*". On the left side there is the X component of displacement, while on the right side the Y component. In Fig. 8, the results from the accelerometers records are reported: the top plot depicts the displacements as calculated from the Acc. "*c*" sensor, while the bottom plot provides the displacements as calculated from the Acc. "*b*" sensor. Also in Fig. 8 the left and right sides show the X component of displacement, and the Y component, respectively.

The two figures confirm a global agreement between the GPS and the accelerometers signals. But the displacements re-elaborated from the accelerometers data show some parts where their amplitude is close to zero and far from the displacement obtained by the GPS units. This confirms once again how the GPS signal is affected by noises produced by a phenomenon known as "Dilution of Precision, which causes the detection of small amplitude displacements even with the structure at rest (Casciati and Fuggini 2009, Fuggini 2010).

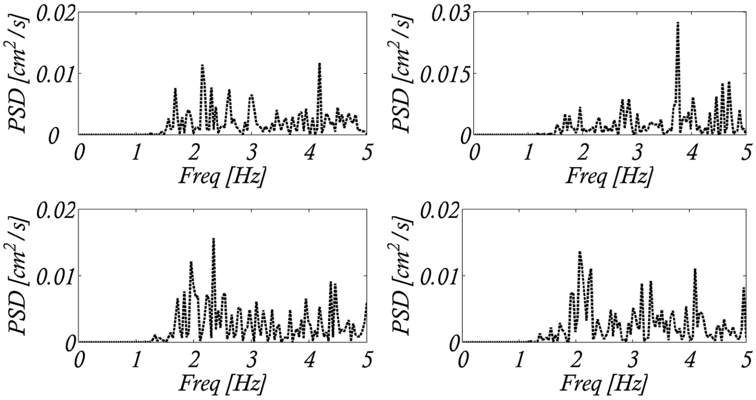

Fig. 9 PSD functions from the GPS measurements along X (left side plots) and Y axes (right side plots), Top: PSD of the GPS unit "*c*". Bottom: PSD of the GPS unit "*b*"

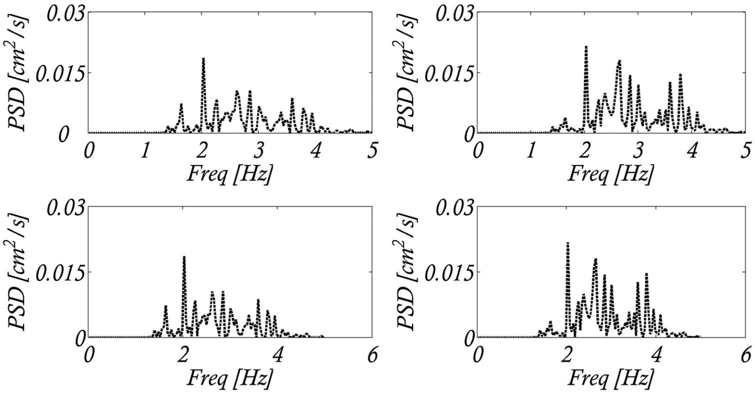

Fig. 10 PSD functions from the accelerometers calculated displacements along X (left side plots) and Y axes (right side plots), Top: PSD of Acc. "*c*" data, Bottom: PSD of Acc. "*b*" data

The comparison of the GPS and accelerometers data is then carried out in the frequency domain where again the same trend is shown for both sensor types, as depicted in Figs. 9 and 10.

From the data recorded by GPS and accelerometers sensors, while the bridge-crain was moving along its rail inside the steel building, a modal identification of the structure was carried on to confirm the agreement in the frequency domain, between the GPS and the accelerometers. The modal identification is conducted by means of the NExT technique (James *et al.* 1995) combined with the ERA method (Juang and Pappa 1985). The NExT-ERA method, suitable for output-only system identification, is adopted to determine the dynamic characteristics (i.e., natural frequency and damping) of the steel buildings from ambient vibrations records of both GPS and accelerometers sensors, for both X and Y components. Free response time domain data from the NExT are used as input for the ERA to estimate the modal properties of a system.

The block Hankel matrix H is constructed from the state space representation. An optimization of its number of rows (r) and columns (c) is pursued. The separation between spurious (i.e., noise) and real (i.e., true) modes is realized based on the stability of the Modal Assurance Criterion (MAC).

"True" modes were selected when:

- Natural frequency variations are within the 10% for a variation of the order of H within the 10%

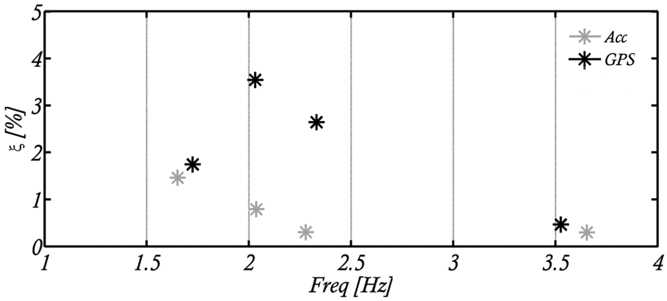

Fig. 11 Stability diagram from GPS unit and accelerometer records

Table 1 Identified natural frequencies from GPS and accelerometers data

	Experimental GPS	Experimental accelerometers	Percentage variation
First mode	1.72Hz	1.65Hz	4,08%
Second mode	2.03Hz	2.07Hz	1,93%
Third mode	2.33Hz	2.27Hz	1,76%
Forth mode	3.52Hz	3.65Hz	3,56%

- MAC values are higher than 0.95
- Damping rations are lower than 5%

A graphical representation of the outcomes from the Next-ERA method is given by means of the stability diagram of Fig. 11. The diagram depicts the correlation between identified natural frequencies and identified damping ratios for both GPS and accelerometers data.

Fig. 11 confirms the GPS and accelerometers agreement in identified the steel building natural frequencies as reported in Table 1 above.

On the contrary, in Fig. 11 the variability of the damping calculated from the GPS data is evidenced in comparison with the damping values derived from the accelerometers data. While for the first and the forth frequency data a good agreement is shown, for the second and third frequency the GPS damping are not so close to the accelerometers damping. This could be caused by two factors: the first is inherent in any OMA methods, which are known to be often affected by uncertainties in the calculation of the modal damping when operating with different data sets and with data recorded by different sensors. Secondly the GPS ability in detecting modal damping has not yet been proved and, maybe, to assess the damping from GPS requires further investigations.

5. Tests with impact and deceleration forces

The calibration process of the parameters of a numerical model of the building and its validation procedure are explained in this section.

The purpose is to identify the main structural parameters and the boundary conditions of the structure and to analyze the way the GPS data have to be processed in the identification scheme.

Attention is manly paid on the longitudinal movements of the bridge-crane which induce significant vibrations in the steel structure.

Two main operations are considered:

a) the bridge-crane moves at a constant speed of 0.7 m/s and is stopped along its way introducing a constant deceleration force F_d of amplitude 10.93 KN for a duration of 0.7 sec

b) the bridge-crane stops by impact at its end, thus introducing an impact force F_i.

While the bridge-crane is moving along the longitudinal direction, the GPS devices on the roof record the consequent oscillations. The *Y* direction displacements, as calculated from the data recorded by GPS unit "*c*", are then compared with the numerical simulation results achieved by an FE model. A parameter refinement is pursued until convergence. When the experimental and the numerical results have matched each the other, the achieved structural model is validated by comparing the numerical response to the internal impact force with the one detected experimentally.

5.1 FE model

A 3D frame FE model of the steel building (Fig. 12) is realized within the Ansys Software (2003) in order to meet two items:

(i) to identify the mode shapes and the natural frequencies of the structure

(ii) to simulate the bridge-crane movements and to estimate the nodal displacements to be compared with the experimental data collected by the GPS units.

The model (see Fig. 12) consists of: (a) Beam elements modelling the steel columns, the perimeter horizontal beam and the roof, (b) Truss elements for modelling the 2D Pratt truss (upper chords, bottom chords, verticals and diagonals elements), the perimeter longitudinal wind-braces and the roof horizontal diagonal-braces and (c) Shell elements for modelling the concrete first and second floor slabs.

5.2 FE model calibration

The model calibration is carried out by considering the excitation case in which the bridge-crane stops on its rails without any impact. This case is represented in the FE environment by the dynamic analysis of the response of the structure subjected to a deceleration force F_d (of 10.93 KN) induced by the bridge-crane, when the along beam motion is suddenly stopped. In the FE model, the action is simulated by considering the bridge-crane as a mass *M* (sum of the crane trolley and crane bridge) of 10145 Kg, moving at a constant speed of 0.7 m/s, stopped in 0.7s.

The main effort in the iterative numerical calibration process (to match the experimental results) is carried out by varying the column bottom constraints, as the uncertainty of the model to be reduced. By iteration, different base constrain conditions had been studied until an agreement with the experimental data, in terms of modal parameters, was reached (see Fig. 11). In particular, the bottom of the columns supporting the bridge-crane rails resulted free to rotate (along the vertical axis),

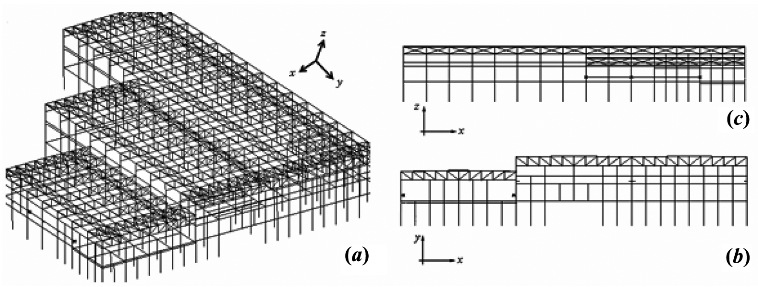

Fig. 12 3D view (a) front view (b) and lateral view (c) of the FE model

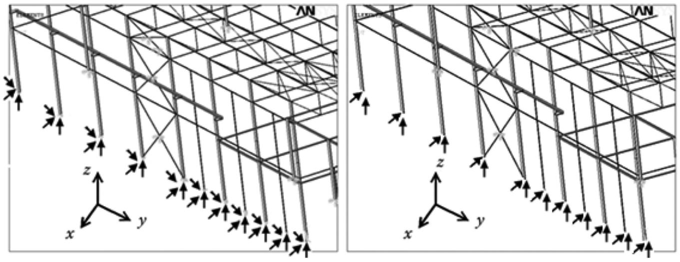

Fig. 13 Details on the constrains of the columns supporting the bridge-crane: fixed supports condition (on the left - case 1); final constraints condition (on the right - case 2)

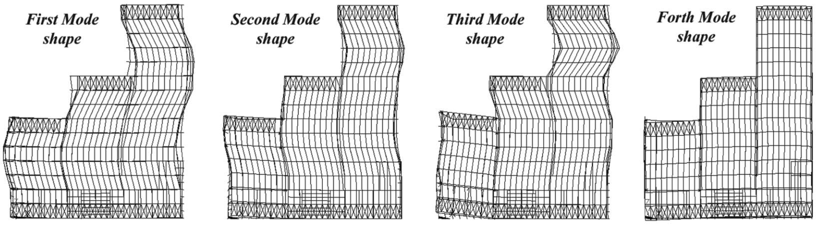

Fig. 14 Numerical mode shapes referring to the final constraints condition (case 2)

Table 2 Experimental and numerical natural frequencies of the building

	Experimental GPS	Experimental accelerometers	Numerical case 1	Numerical case 2
First mode	1.72Hz	1.65Hz	1.57Hz	1.55Hz
Second mode	2.03Hz	2.07Hz	1.92Hz	1.95Hz
Third mode	2.33Hz	2.27Hz	/	2.24Hz
Forth mode	3.52Hz	3.65Hz	3.52Hz	3.49Hz

while the displacements along X and along Z were not allowed.

Fig. 13 reports the initial constrains model configuration named as case 1 (on the left) and the final (calibrated) one named as case 2 (on the right).

The results from a modal analysis (see Fig. 14) provide a validation of the procedure pursued in the model calibration.

The values of the experimental and the numerical natural frequencies associated to the first forth mode shapes are reported in Table 2, where for the numerical analysis the two aforementioned cases are represented.

Table 2 suggests a good agreement between the experimental and numerical frequencies, allowing proceeding further in the comparison of the response of the structure when subjected to the deceleration force. It is presented in Fig. 15, which shows the experimental time history displacement recorded by the GPS receiver "c" and the displacement time history in the same position as numerically simulated.

A further dynamic analysis is carried out to study the behaviour of the structure subjected to repetitive decelerations of the bridge-crane. The numerical solution is calculated by reproducing the condition of the bridge-crane consecutively accelerated and decelerated, inducing, at each discontinuity time, an acceleration force F_a and a deceleration force F_d (Fig. 16).

In the FE model these actions are again generated considering the bridge-crane as a mass of 10145 Kg, which accelerate with a constant acceleration of 0.49 m/s^2, moving at a constant speed of

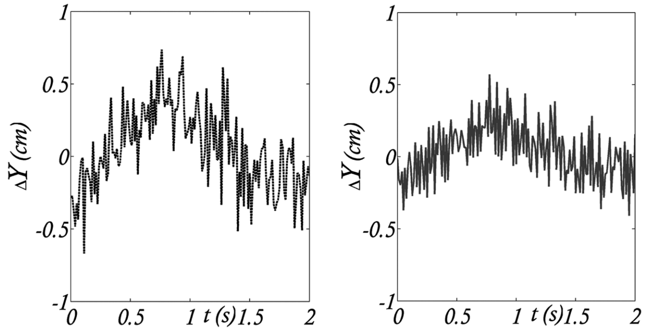

Fig. 15 Test under the deceleration force induced by the bridge-crane: experimental results from GPS receiver "*c*" data (left), numerical results (right)

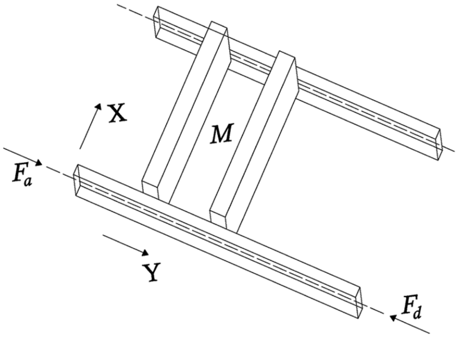

Fig. 16 Scheme of bridge-crane forces during vibration tests

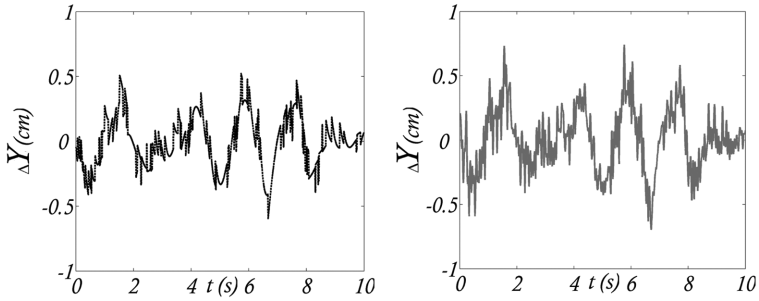

Fig. 17 Structural Displacement of the deceleration-acceleration force: experimental results from GPS receiver "*c*" data (left), numerical results (right)

0.7 m/s and then stopping in 0.7 s.

Fig. 17 shows the experimental time history displacement recorded by the GPS receiver "*c*" and the displacement time history which was numerically simulated in the same position.

5.3 FE model validation

The validation of the structural model is conducted by using another input action, which considers as input action the impact force F_i produced when the bridge-crane impacts at its end. The force is simulated in the FE environment as an application of the impulse theorem as

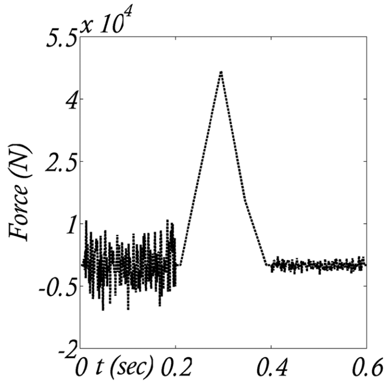

Fig. 18 Calculated FE model input impact force

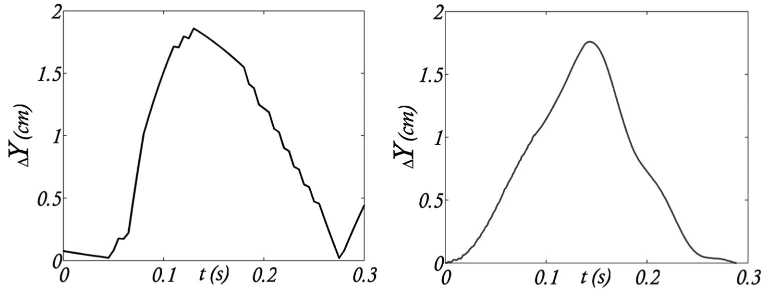

Fig. 19 Impact force: experimental results from GPS receiver "*c*" (left), numerical results (right)

presented below

$$I = mv_f - mv_i = \int_{t_i}^{t_f} F_i(t)dt \Rightarrow \frac{for\ a\ given}{pulse\ shape} \Rightarrow F_{i(max)} \tag{3}$$

After different attempts to calibrate it by a trial and error procedure, the impact force is calculated as plotted in Fig. 18. Note that a white noise signal is added before and after the application of the impact force simulating the bridge-crane movements along its beam way.

The resulting impact force produces displacements which are about three times greater than those induced by the deceleration force. Fig. 19 shows the experimental and numerical displacements time histories referred to the node of the GPS unit receiver "*c*". The comparison validates the numerical model built and calibrated above in this section.

6. Conclusions

The use of GPS units for structural monitoring is discussed in this contribution.

The effectiveness of a full-scale implementation is investigated. The steel building which host the authors' laboratory is chosen as the case study. Man made dynamic actions are considered to excite the structure. The ability of GPS sensors to detect the response of the structure to pulse actions (short duration actions) as the movements of the bridge-crane inside the building is assessed.

The potential offered by the GPS approach for monitoring the dynamic displacements is emphasized by comparing, both in the time and the frequency domains, the displacements measured by the GPS units with the displacements re-elaborated from tri-axial accelerometers data.

The refinement of the parameters of the numerical model of the building is then pursued from the GPS recorded signals. The identification/validation process exploits the structural response to movements of the internal bridge-crane. A FE model of the steel building is conceived and refined. The simulations are carried out in two different scenarios of dynamical excitation induced by the bridge-crane. The agreement of experimental and numerical results in the two independent cases validates the FE model.

Acknoledgements

The authors acknowledge the GPS installation and the technical support as provided by the company Leica Geosystems. The research was supported by a grant from the University of Pavia (FAR 2009).

References

Sumitro, S. and Wang, M.L. (2005), "Sustainable structural health monitoring system", *Struct. Health Monit.*, **12**(3-4), 445-467.

Celebi, M. (2000), "GPS in dynamic monitoring of long-period structures", *Soil Dyn. Earthq. Eng.*, **20**(5-8), 477-483.

Nickitopoulou, A., Protopsalti, K. and Stiros, S. (2006), "Monitoring dynamic and quasi-static deformations of large flexible engineering structures with GPS: accuracy, limitations and promises", *Eng. Struct.*, **28**(10), 1471-1482.

Kijewsji-Correa, T., Kareem, A. and Kochly, M. (2006), "Experimental verification and full-scale deployment of global positioning systems to monitor the dynamic response of tall buildings", *J. Struct. Eng.*, **132**(8), 1242-1253.

Li, X., Ge, L., Ambikairajah, E., Rizos, C., Tamura, Y. and Yoshida, A. (2006), "Full-scale structural monitoring using an integrated GPS and accelerometer system", *GPS Solut.*, **10**(4), 233-247.

Psimoulis, P., Pytharouli, S., Karambalis, D. and Stiros, S. (2008), "Potential of global positioning system (GPS) to measure the frequencies of oscillations of engineering structures", *J. Sound Vib.*, **318**(3), 606-623.

Kijewsji-Correa, T.L. and Kareem, A. (2003), "The Chicago monitoring project: a fusion of information technologies and advanced sensing for civil infrastructures", *Proceedings of the 1thInternational Conference on Structural Health Monitoring and Intelligent Infrastructure*, Tokyo, November.

Campbell, S. Kwok, K.C.S., Keung, Y.L. and Hitchcock, P.A. (2006), "Full-scale monitoring of a high-residential building using GPS under typhoon conditions", *Proceedings of the 4th World Conference on Structural Control and Monitoring*, San Diego, July.

Seco, A. Tirapu, F., Ramirez, F., Garcia, B. and Cabrejas, J. (2007), "Assessing building displacement with GPS", *Build. Environ.*, **42**(1), 393-399.

Hristopulos, D.T., Mertikas, S.P., Arhontakis, I and Brownjohn, J.M.W. (2007), "Using GPS for monitoring tall-building response to wind loading: filtering of abrupt changes and low-frequency noise, variography and spectral analysis of displacements", *GPS Solut.*, **11**(2), 85-95.

Xu, L., Guo, J.J. and Jiang, J.J. (2002), "Time-frequency analysis of a suspension bridge based on GPS", *J. Sound Vib.*, **254**(1), 105-116.

Lekidis, V., Tsakiria, M., Makrab, K., Karakostasb, C., Klimisb, N. and Sous, I. (2005), "Evaluation of dynamic response and local soil effects of the Evripos cable-stayed bridge using multi-sensor monitoring systems", *Eng. Geol.*, **79**(1-2), 43-59.

Meng, X., Dodson, A.H. and Roberts G.W. (2007), "Detecting bridge dynamics with GPS and triaxial accelerometers", *Eng. Struct.*, **29**(11), 3178-318.

Breuer, P., Chmielewski, T., Gorski, P. and Konopka, E. (2002), "Application of GPS technology to measurements of displacements of high-rise structures due to weak winds", *J. Wind Eng. Ind. Aerod.*, **90**(3), 223-230.

Cazzaniga, N.E. and Pinto, L. (2006), "Structural monitoring with GPS and accelerometers: the chimney of the power plant in Piacenza", *Proceedings of the 3rd IAG Symposium on Geodesy for Geotechnical and Structural Engineering and 12th FIG Symposium on Deformation Measurements*, Baden, May.

Barnes, J. and Cranenbroeck, J. V. (2006), "The potential of a ground based transceivers network for water dam deformation monitoring", *Proceedings of the International Conference Hydropower*, Kunming, October.

Tamura, Y., Matsui, M., Pagnini, L. C., Ishibashi, R. and Yoshida, A. (2002), "Measurement of wind induced response of building using RTK-GPS", *J. wind eng. Ind. Aerod.*, **90**(12-15), 1783-1793.

Wong, K.Y. (2004), "Instrumentation and health monitoring of cable-supported bridges", *Struct. Control Health Monit.*, **11**(2), 91-124.

Psimoulis, P. and Stiros, S. (2008), "Experimental assessment of the accuracy of GPS and RTS for the determination of the parameters of oscillation of major structures", *Comput. Aided Civil Infrastruct. Eng.*, **23**(5), 389-403.

Ni, Y.Q., Xia, Y., Liao, W.Y. and Ko, J.M. (2009), "Technology innovation in developing the structural health monitoring system for Guangzhou New TV Tower, *Struct. Control Health Monit.*, **16**(1), 73-98.

Casciati, F. and Fuggini, C. (2009), "Engineering vibration monitoring by GPS: long duration records", *Earthq. Eng. Eng. Vib.*, **8**(3), 459-467.

Casciati, F. and Fuggini, C. (2009), "Towards global positioning system-based structural health Monitoring, in B. H.V. Topping, L.F. Costa Neves, R.C. Barros (editors), Trends in Civil and Structural Engineering Computing, Saxe Coburg Pubblications, Stirlingshire, Scotland, 319-352.

Leica (2005), GMX 902 User Manual. Leica Geosystems AG.

Matlab, The MathWork Inc., Version 7 (R14), 2004.

Dana, P.H. (1997), "Global positioning system (GPS) time dissemination for real-time applications, real-time systems", *Int. J. Time Critical Comput. Syst.*, **12**(1), 9-40.

Casciati, F., Fuggini, C. and Bonanno C. (2007), "Dual frequency GPS receivers: reliability of precision of the measures", *Proceedings of the 4me Colloque en Interdisciplinaire en Instrumentation C2I*, Hermes Science, Paris, France.

Casciati, F. and Fuggini, C. (2008), "Measuring the displacements of a steel structure by GPS units", *Proceedings of the 1st International Symposium on Life-Cycle Engineering*, Varenna.

Casciati, F. and Fuggini, C. (2008), "Monitoring an industrial steel building by GPS receivers", *Proceedings of the 4th European Workshop on Structural Health Monitoring*, Krakow.

Casciati, F. and Fuggini, C. (2008), "GPS based structural identification and health monitoring", *Proceedings of the 4th European Conference on Structural Control*, St. Petersburg.

Kaplan, E. and Hegarty, C. (2006), "Understanding GPS principles and applications", Artech House, Boston, 2nd edition.

Fuggini, C. (2010), "*Using satellites systems for structural monitoring: accuracy, uncertainty and reliability*", PhD Dissertation, University of Pavia, Pavia, Italy.

James, G.H., Carne, T.G. and Lauffer, J.P. (1995), "The natural excitation technique (NExT) for modal parameter extraction from operating structures", *Int. J. Analytical Experimental Modal Anal.*, **10**(4), 260-277.

Juang, J.N. and Pappa, R.S. (1985), "An eigensystem realization algorithm for modal parameter identification and model reduction", *J. Guid. Control Dynam.,* **8**(5), 620-627.

ANSYS Users Manual, ANSYS Inc, 2003.

BS